Electronic Supplementary Material (ESI) for Journal of Materials Chemistry A.

Supporting Information

Solvent-Induced Surface Disorder and Doping-Induced Lattice Distortion in Anatase TiO_2 Nanocrystals for Enhanced Photoreversible Color Switching

Kewei Yang,[a] Xiaoyu Chen,[a] Zhenhuan Zheng,[a] Jiaqi Wan,[a] Miao Feng, [*a, b] and Yan Yu [*a, b]

[a] *College of Materials Science and Engineering, Fuzhou University, 2 Xueyuan Road, Fuzhou, Fujian, 350116, China.*

[b] *Key Laboratory of Eco-Materials Advanced Technology, Fuzhou University, 2 Xueyuan Road, Fuzhou 350116, China.*

* Corresponding author.

E-mail addresses: mfeng@fzu.edu.cn (M. Feng), yuyan@fzu.edu.cn (Y. Yu).

ORCID

Miao Feng: 0000-0003-4378-803X

Yan Yu: 0000-0001-6748-2620

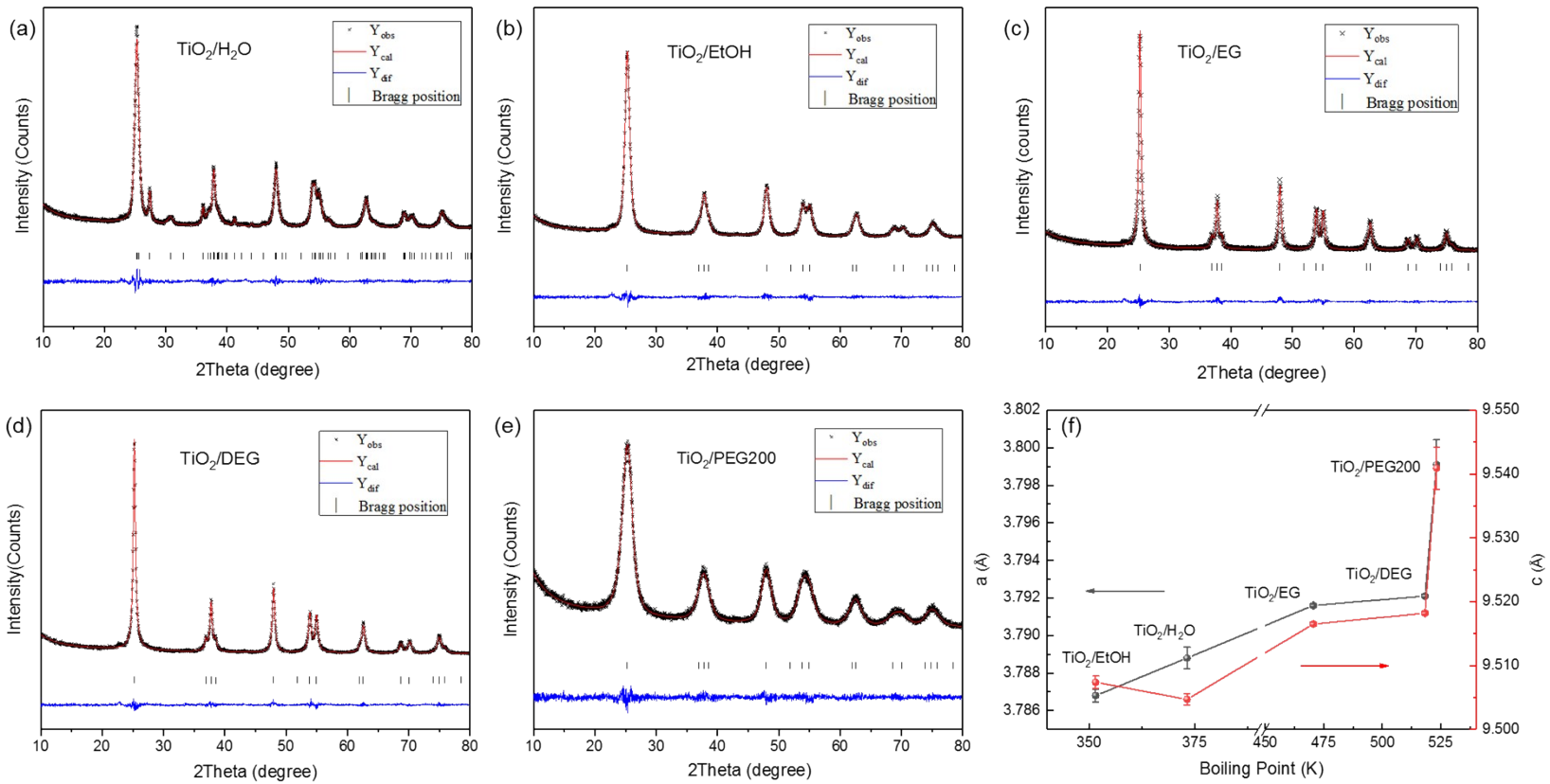

Fig. S1 Rietveled refined XRD patterns for TiO_2/H_2O (a), TiO_2/EtOH (b), TiO_2/EG (c), TiO_2/DEG (d), and TiO_2/PEG200 (e). Black cross stand for the observed value, red line represents the fitting line, blue curve is the difference of observed and the calculated curve and black bar is the peak position. (f) Boiling point of the solvent dependences of the lattice parameter *a*, *c* values for TiO_2 NCs.

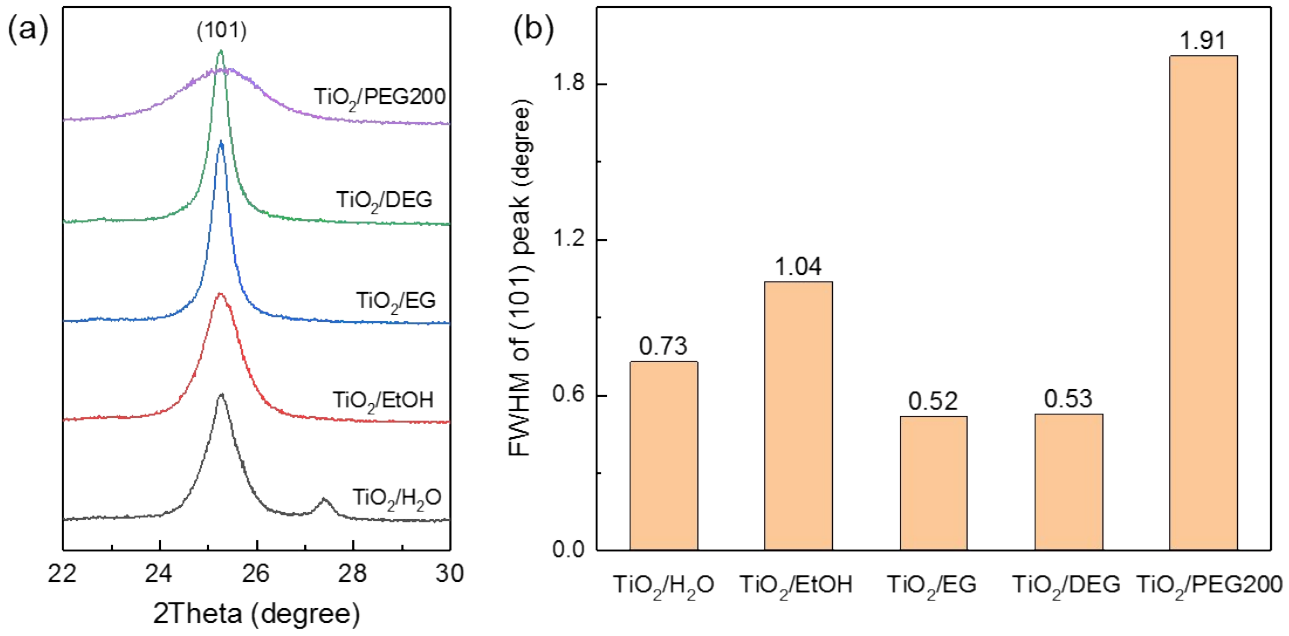

Fig. S2 (a) Enlarged XRD patterns and (b) FWHM value of (101) peak of all the samples.

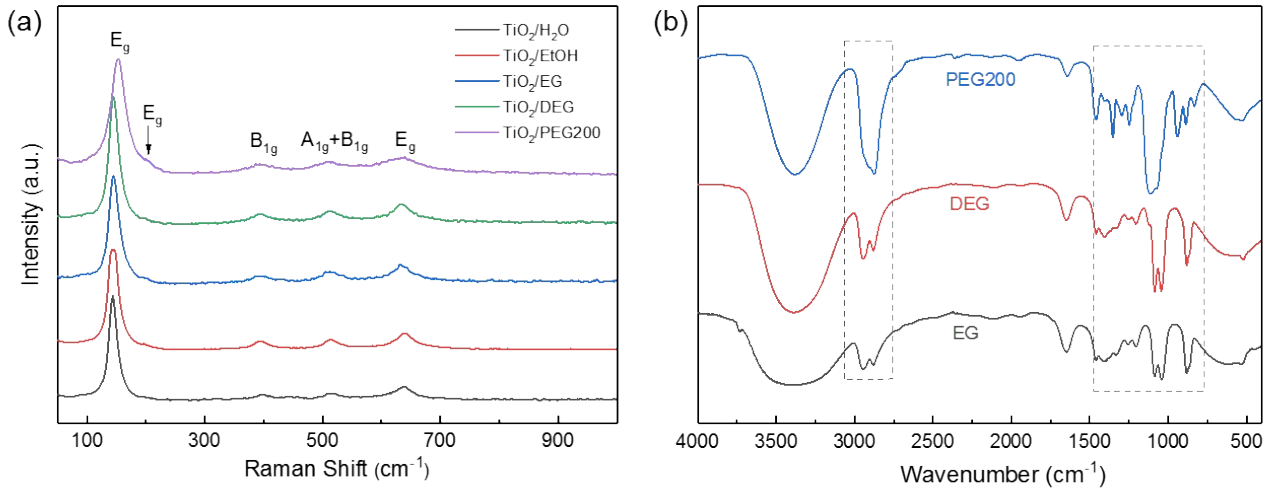

Fig. S3 (a) Raman spectra of TiO_2 NCs synthesized in different solvents. (b) FT-IR spectra of EG, DEG, PEG200.

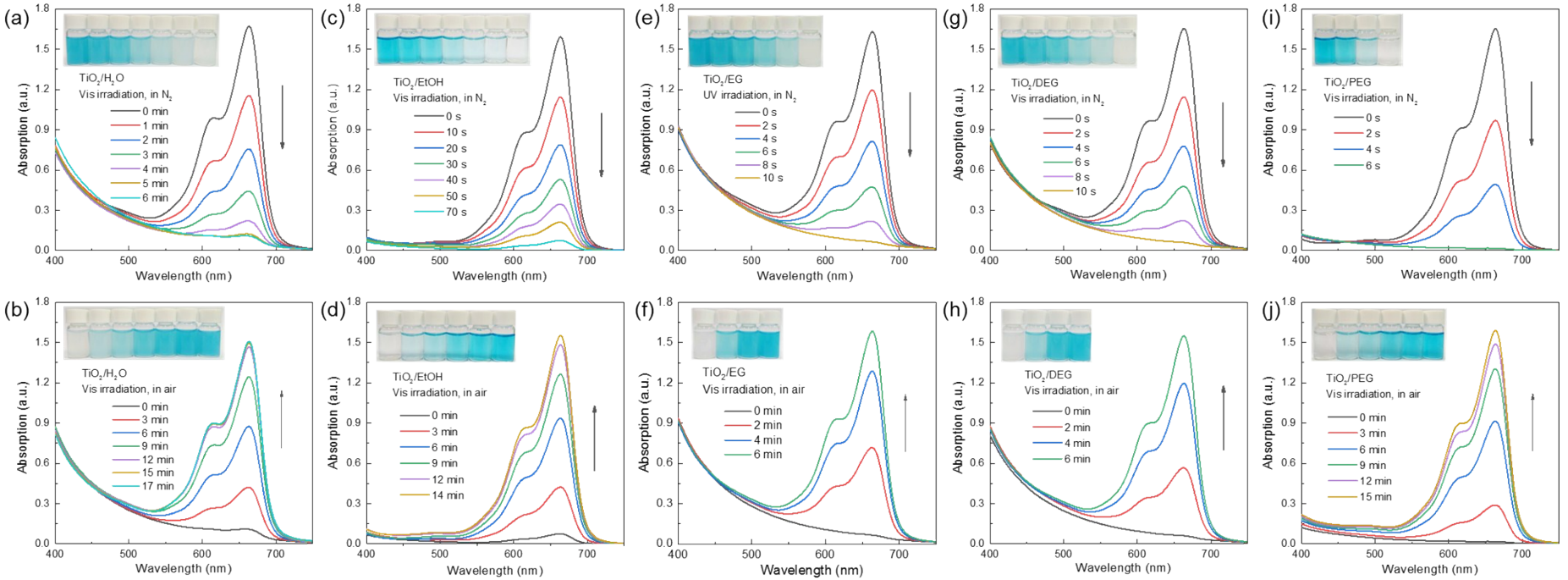

Fig. S4 The decoloration and recoloraion process of the TiO_2/MB/H_2O system: (a, b) TiO_2/H_2O, (c, d) TiO_2/EtOH, (e, f) TiO_2/EG, (g, h) TiO_2/DEG, and (i, j) TiO_2/PEG200.

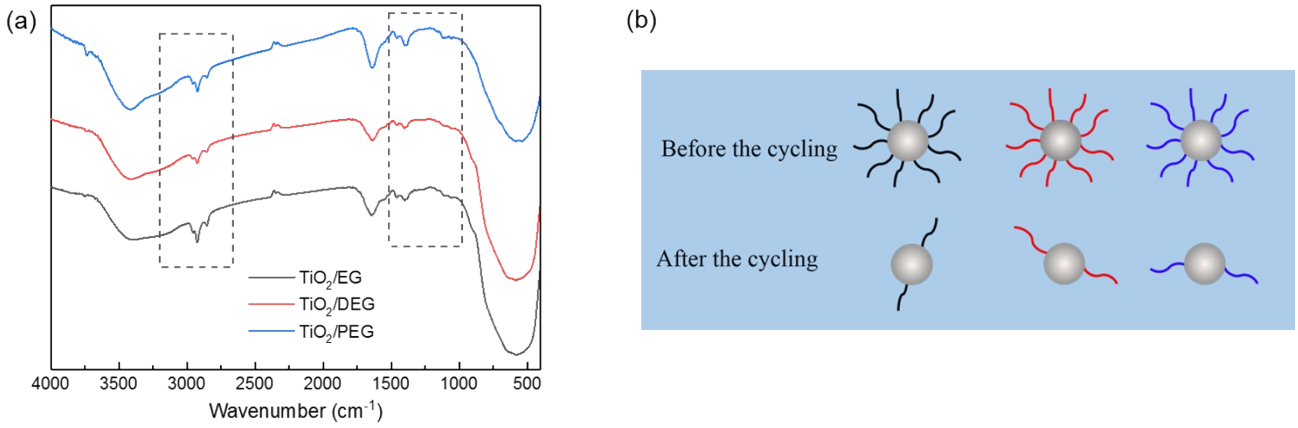

Fig. S5 (a) FT-IR spectra of TiO_2/EG, TiO_2/DEG, TiO_2/PEG200 after cycling. (b) Schematic illustration of the change of surface functional groups of TiO_2 NCs.

Table S1 Parameters related to the lattice of TiO_2/H_2O, TiO_2/EtOH, TiO_2/EG, TiO_2/DEG, TiO_2/PEG200 NCs determined by linear fit of the Halder-Wagner plot.

Samples	Crystalline size (nm)	Linear fit of the Halder-Wagner plot		R value
		Slope	Y intercepts	
TiO_2/H_2O	11.4	1.1598 ± 0.39314	0.01389 ± 0.02205	0.96501
TiO_2/EtOH	9.3	1.22686 ± 0.11524	0.01273 ± 0.00743	0.99273
TiO_2/EG	19.8	0.6701 ± 0.128	0.00479 ± 0.00447	0.98409
TiO_2/DEG	19.7	0.65286 ± 0.11237	0.00516 ± 0.00392	0.98773
TiO_2/PEG200	4.4	2.67788 ± 0.24131	0.00295 ± 0.02972	0.99351

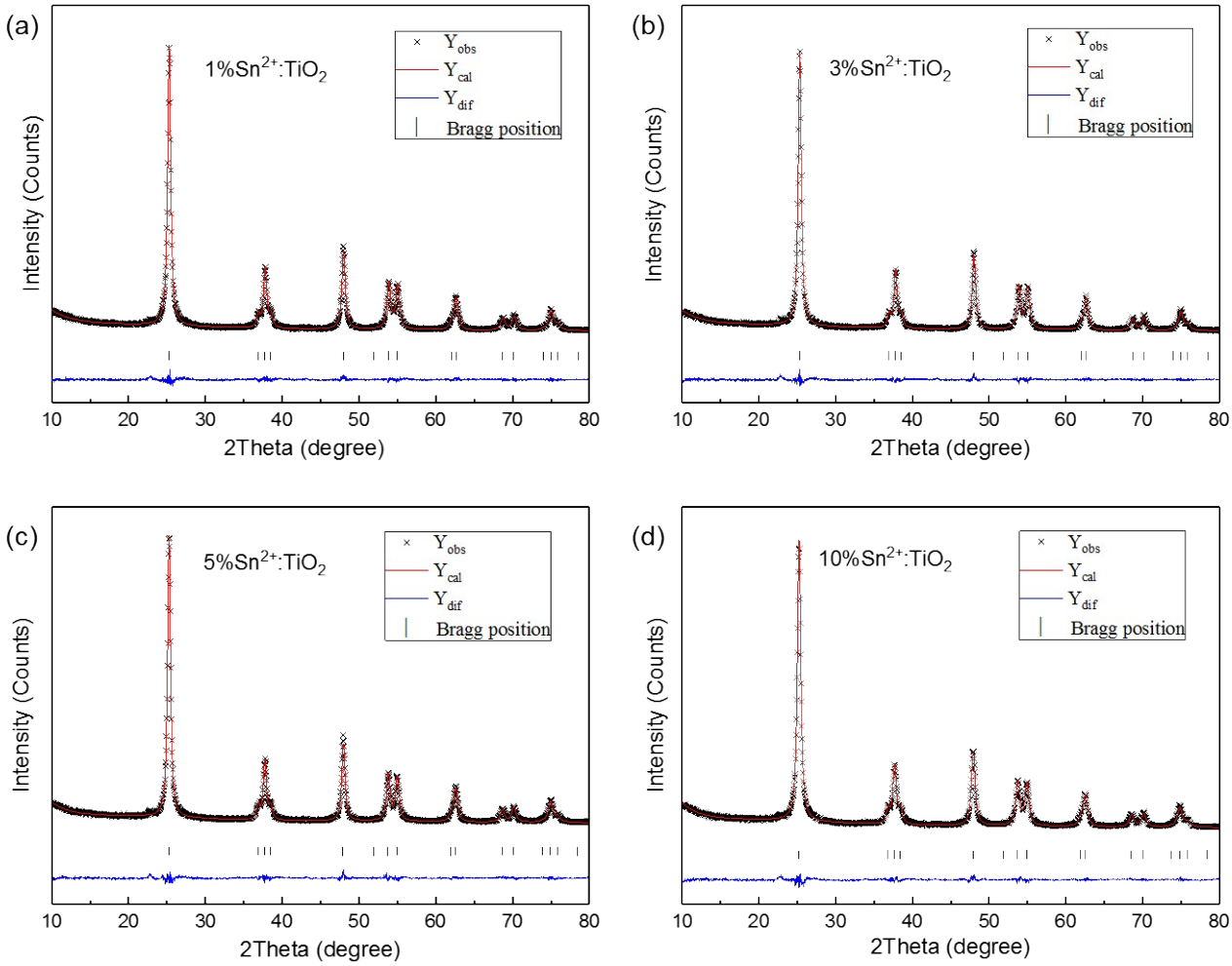

Fig. S6 Rietveled refined XRD patterns of (a) 1%Sn^{2+}:TiO_2, (b) 3%Sn^{2+}:TiO_2, (c) 5%Sn^{2+}:TiO_2, and (d) 10%Sn^{2+}:TiO_2. Black cross stands for the observed value, red line represents the fitting line, blue curve is the difference of observed and the calculated curve and black bar is the peak position.

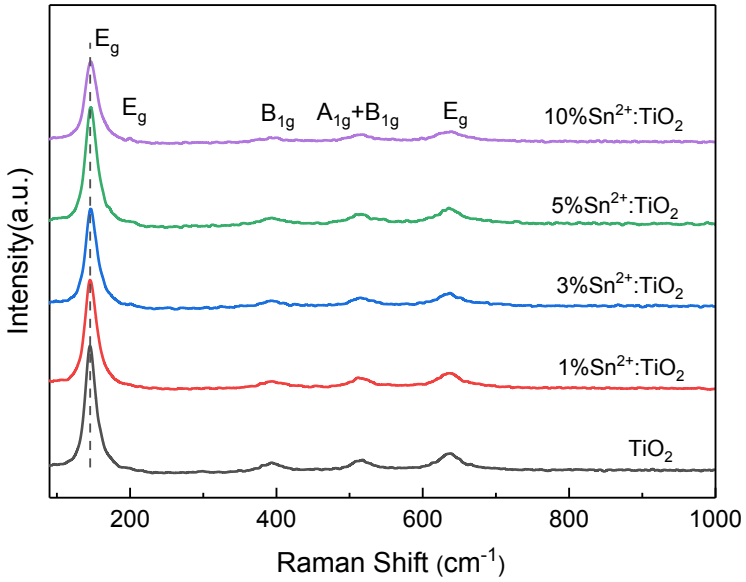

Fig. S7 Raman spectra of Sn^{2+} :TiO_2 NCs having different doping concentrations.

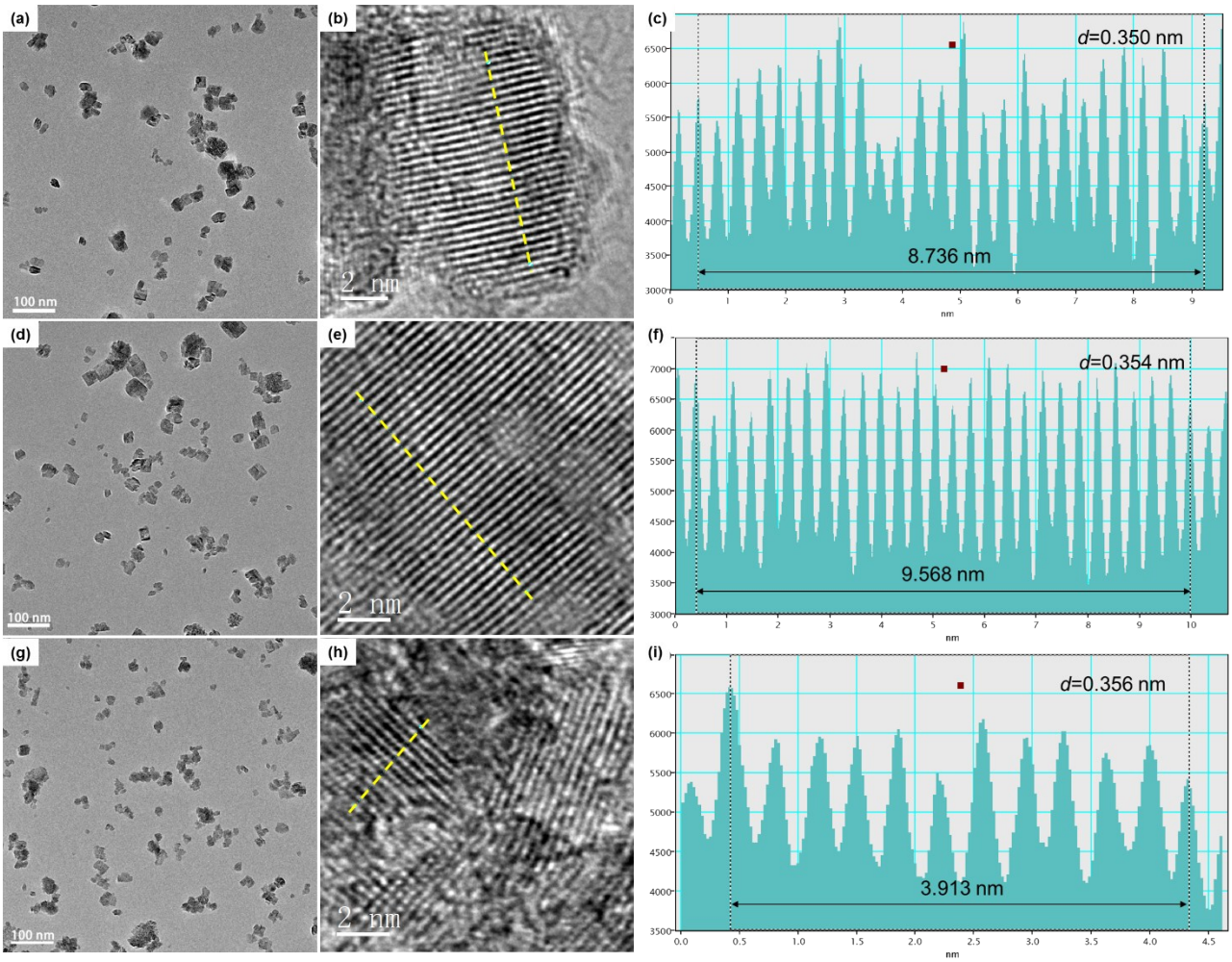

Fig. S8 Low-magnification TEM patterns of (a) TiO_2 NCs, (d) 3% Sn^{2+}:TiO_2 NCs and (g)10% Sn^{2+}:TiO_2 NCs. Intensity line profile (c), (f) and (i) extracted from the HRTEM images of (b)TiO_2 NCs, (e) 3% Sn^{2+}:TiO_2 NCs, and (h) 10% Sn^{2+}:TiO_2 NCs.

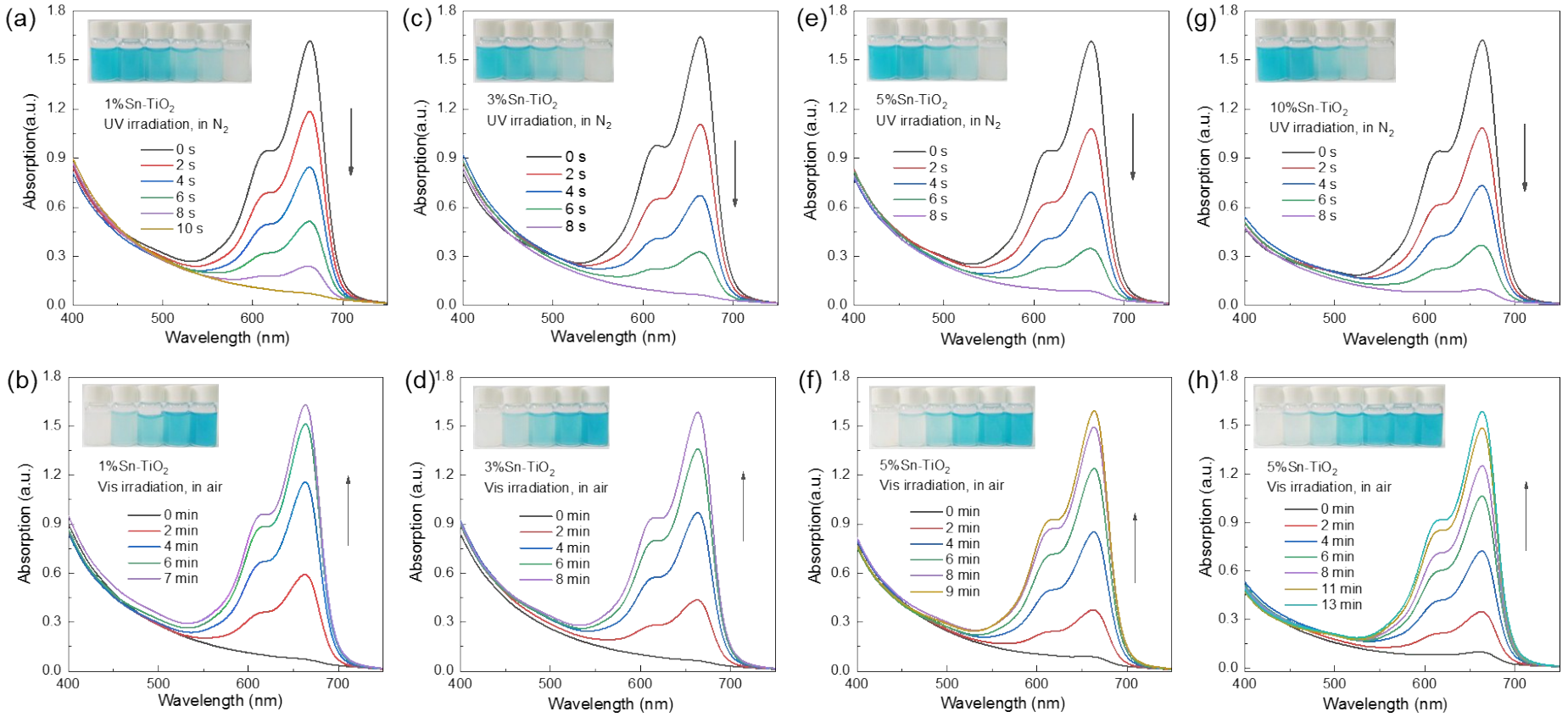

Fig. S9 The decoloration and recoloraion process of Sn^{2+} doped TiO_2/MB/H_2O system: (a, b) 1%Sn^{2+}:TiO_2, (c, d) 3%Sn^{2+}:TiO_2, (e, f) 5%Sn^{2+}:TiO_2, and (g, h) 10%Sn^{2+}:TiO_2.

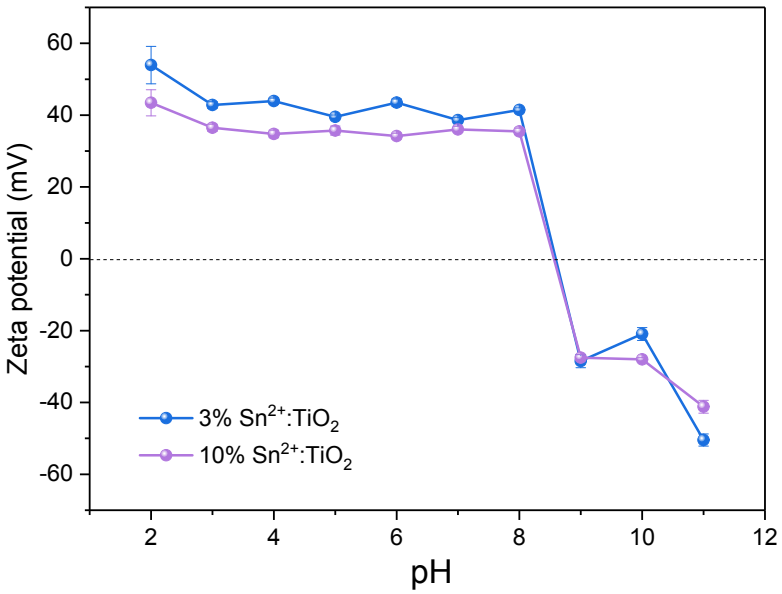

Fig. S10 Diagram of the relationship between the change of Zeta potential and the solution system with different pH values of 3%Sn^{2+}:TiO_2 and 10% Sn^{2+}:TiO_2.